Experimental Spectroscopy II

H.-J. Kunze

Institute for Experimental Physics V, Ruhr-University,
44780 Bochum, Germany

Joint ICTP-IAEA School on Atomic Processes in Plasmas
Trieste, February 27 to March 3, 2017

Prerequisite for diagnostic applications is the knowledge of

excellent atomic data

obtained from experiments and/or

from theoretical calculations

supplemented by theoretical descriptions/simulations of the behavior and the emission of atomic species in plasmas

For the derivation of such data from spectroscopic observations on plasmas one needs a plasma well diagnosed, preferably by other methods.
This can be, for example:

- Thomson scattering employing lasers
- Electric probes in case of low-temperature plasmas
- Interferometry and polarimetry
- Other well established spectroscopic techniques
- based on well-known data

In the following we assume,

that from the absolute measured radiance L_z of a line an *absolute local* emission coefficient $\varepsilon_z(\mathbf{r})$ is derived !

The fundamental equation for the line emission from an upper level p to a lower level q is given by

$$\varepsilon_z(p \to q) = \frac{h\nu_{pq}}{4\pi} A_z(p \to q)\, n_z(p) \qquad \left[\frac{W}{m^3 sr}\right]$$

where $h\nu_{pq}$ is the photon energy

$A_z(p \to q)$ is the transition probability and

$n_z(p)$ is the population density of the upper level

z is the charge of the ion

Measurement of Particle Densities

Particle Densities from Absolutely Measured Line Emission

$$n_z(p) = \frac{4\pi\, \varepsilon_z(p \to q)}{h\nu_{pq}\, A_z(p \to q)}$$

The quantity obtained is the population density of the upper level !!!

In the limit of LTE (local thermodynamic equilibrium, electron collisions between all levels are fast to establish equilibrium) the total density n_z of all the levels of the ion including its ground state is given by

$$n_z = n_z(\mathrm{p}) \frac{U_z(T_e)}{g_z(p)} \exp\left[\frac{h\nu_{pq}}{k_B T_e}\right]$$

$g_z(p)$ statistical weight of upper level

$U_z(T_e)$ partition function of the ion

Electron temperature T_e must be known and the partition function of the ion must be available

LTE is usually reached at high densities

If LTE is not reached for all levels of an ion or atom, high-lying levels (*p*) can be in collisional equilibrium with the ground-state (g) of the next ion, (PLTE), and its density $n_{z+1}(g)$ can be retrieved

Difficulty:

Both levels are connected by the Saha-Eggert equation and now both electron density and temperature must be known !!!

Another limit are plasmas of sufficiently low electron density

Excitation of upper levels is essentially only by electron collisions from the ground-state of each ion

$$n_z(g)\, n_e\, X_z(g \rightarrow p; T_e) = A_z(p \rightarrow)\, n_z(p),$$

known as coronal excitation equilibrium

$X_z(g \rightarrow p; T_e)$: rate coefficient for collisional excitation from the ground-state (*g*) to level (*p*)

$$n_z \cong n_z(g) = \frac{A_z(p\rightarrow)}{n_e X_z(g\rightarrow p;T_e)}\; n_z(p)$$

Electron density, electron temperature and collisional excitation rate coefficient must be known !

Special case in fusion plasmas:

Magnetic dipole transitions of the type M-1 between the fine structure levels of the ground state of highly ionized species (examples are the green and red iron lines emitted by FeXIV and FeV from the solar corona)

Electron and proton collisions between the fine structure levels are so fast that these levels are in PLTE.
Hence the population densities of these levels and thus the total density of the ion are obtained directly !

Most lines are in the visible and near ultraviolet (*great advantage*!)

Their transition probabilities are small,
but the ground state levels have a high population density,
hence the lines are observable

Particle Densities by Employing Injected Fast Beams

Actinometry

It is increasingly applied to *plasmas containing reactive species*; because of the large number of participating processes with mostly unknown reaction rates any modelling is extremely difficult.

Principile: a gas, the *actinomer*, with well-known excitation characteristics is added at a well-known but low concentration n_{act}, and one measures the intensity ratio of a suitable actinomer line and of a transition in the atom, molecule or ion.

In the low density limit the corona approximation holds and

$$\boxed{\frac{n_x}{n_{act}} = \text{const}\,\frac{\varepsilon_x}{\varepsilon_{act}}\,\frac{X_{act}(T_e)}{X_x(T_e)}}$$

If excitation energies of both lines are about equal, T_e dependence drops out in the ratio.

In general, collisional-radiative models must be employed for both species
and most actinometric systems have been even calibrated by other methods.

Temperature Measurements

Atom, Molecule and Ion Temperature

In general, broadening and shift of recorded spectral lines are determined by
Natural broadening
Pressure broadening by neutral particles
Broadening by Stark and Zeeman effect,
Doppler broadening
Broadening by the instrument function

If some contributions are small and Doppler broadening dominates, deconvolution is possible and the profile mirrors exactly the velocity distribution function of the particles, i.e. their temperature T_a.

Doppler width: $$\frac{\Delta\lambda^G_{1/2}}{\lambda_{pq}} = 7.715 \times 10^{-5} \sqrt{\frac{k_B T_a/\mathrm{eV}}{m_a/\mathrm{u}}}$$

Largest effect on ions of low mass m_a

Electron temperature

Line ratios

Two lines with the population densities of their upper levels p and p' being in PLTE (*coupled by electron collisons*)

$$R = \frac{\epsilon_Z(p\to q)}{\epsilon_Z(p'\to q')} = \frac{\lambda_{p'q'}}{\lambda_{pq}} \frac{A_Z(p\to q)}{A_Z(p'\to q')} \underbrace{\frac{g_Z(p)}{g_Z(p')} \exp\left[-\frac{E_Z(p)-E_Z(p')}{k_B T_e}\right]}_{\text{Boltzmann factor}}$$

Accuracy

$$\frac{\Delta T_e}{T_e} = \frac{k_B T_e}{E_Z(p)-E_Z(p')} \frac{\Delta R}{R}$$

Spacing in energy of upper levels should be large !

Observing several lines increases the accuracy $\rightarrow$ log-plot of the population densities versus $E_Z(p)$ gives a straight line:

$\rightarrow$ Boltzmann plot

Attention: Check if PLTE condition exits,
if a line is optically thick,
in strongly transient plasmas upward or downward excitation flow may result in different distributions of of population densities !!!!!

Molecules: Population densities of rotational and vibrational levels derived from line emission are usually characterized by rotational and vibrational temperatures by fitting a Boltzmann plot
T_{rot} and T_{vib} are formally defined and may differ strongly from T_e.

Excitation temperature T_{exc}:
it is often quoted for technical plasmas. and desribes quite formally the population distribution of excited levels obtained from a Boltzmann plot independently if LTE holds or not.

Ratio of lines from consecutive ionization stages

In LTE

$$R = \frac{\epsilon_{z+1}(p \rightarrow q)}{\epsilon_z(p' \rightarrow q')} \sim \frac{(k_B T_e)^{3/2}}{n_e} \; exp\left[-\frac{E_{z+1}(p) - E_z(p')}{k_B T_e}\right]$$

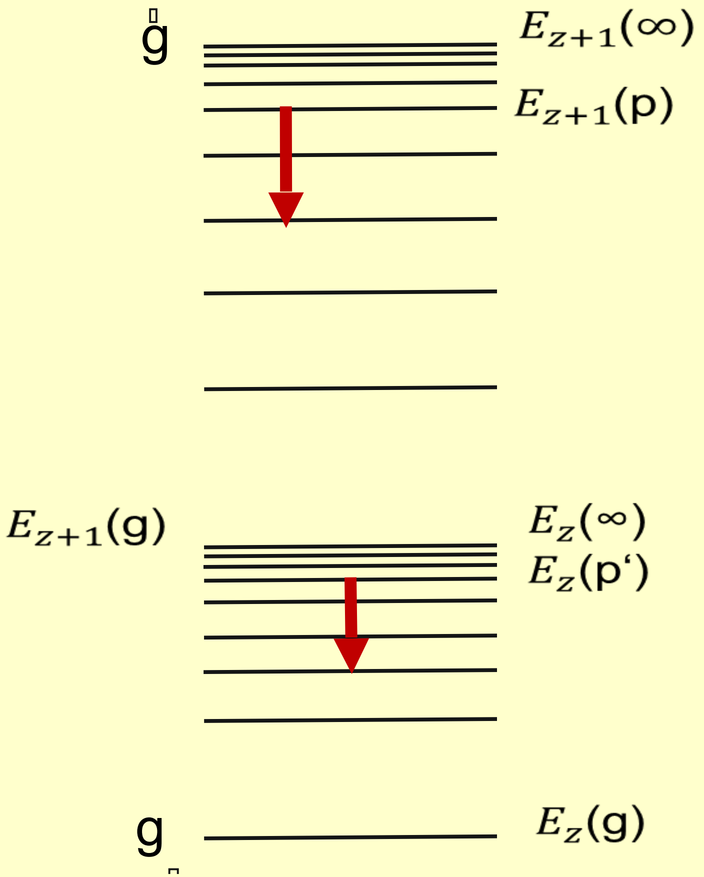

Now the energy difference of the upper levels is larger but a density dependence enters because both ions are connected by the Saha-Eggert equation

It is rarely the case, only at very high densities between atom and first ion

Other cases, for example:

Two upper levels of successive ionization stages are in PLTE with the ground-state of their next ion and both ground-states are in coronal ionization equilibrium

etc

At low electron densities the coronal model holds,
i.e. excitation by electron collisions from the ground state and decay by radiation

$$R = \frac{\varepsilon_Z(p\rightarrow q)}{\varepsilon_Z(p'\rightarrow q')} = \frac{\lambda_{p'q'}}{\lambda_{pq}} \frac{A_Z(p\rightarrow q)}{A_Z(p\rightarrow)} \frac{A_Z(p'\rightarrow)}{A_Z(p'\rightarrow q')} \frac{X_Z(T_e;g\rightarrow p)}{X_Z(T_e;g\rightarrow p')}$$
$$= f_Z(T_e)$$

The ratio is a sole function of T_e

If excitation is by a dipole transition,

excitation rate coefficients X_z can be obtained in the effective Gaunt factor approximation

Also here one should select lines with a large energy spacing of the upper levels

Lithium-like ions are a good example:

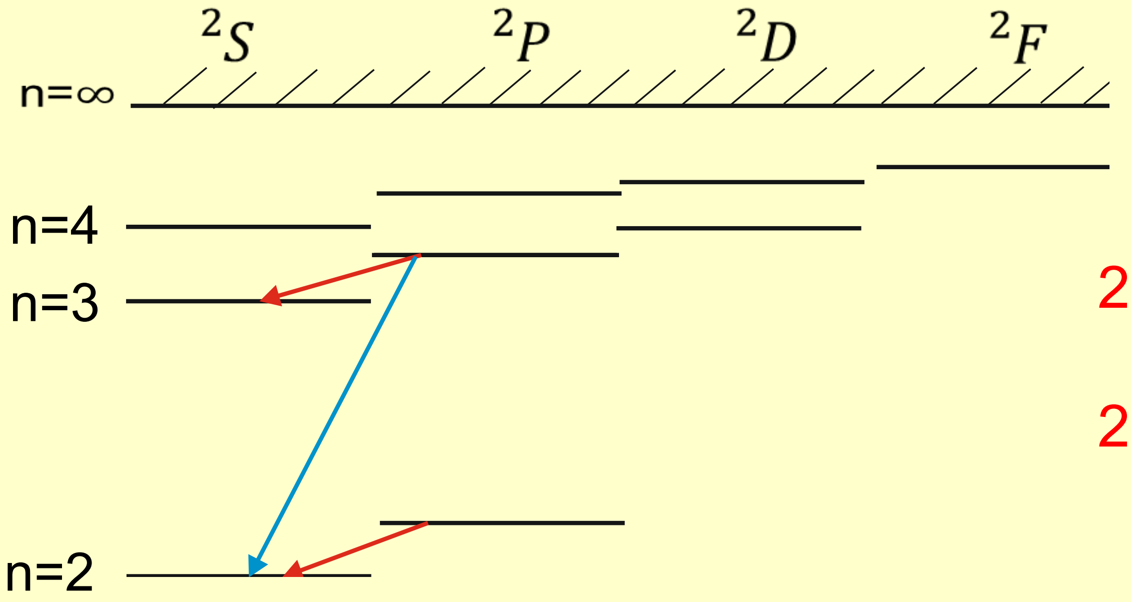

2p → 2s and 3p → 2s

2p → 2s and 3p → 3s

The pair 3p → 3s and 3p → 2s
is even well suited for the branching ratio calibration at short wavelengths; since the 3p → 3s transitions are at long wavelengths the lines are in the UV and visible !

For example: Ne 286 nm NV 461 nm
OVI 381 nm

With increasing density the dependence of line ratios on plasma parameters becomes more complex,

especially if metastable levels are involved which will be highly populated !

Spectra of neutral helium demand special attention due to the longelivity of the metastable levels.
At very low densities they even depopulate by collisions with other atoms and molcules and with the walls

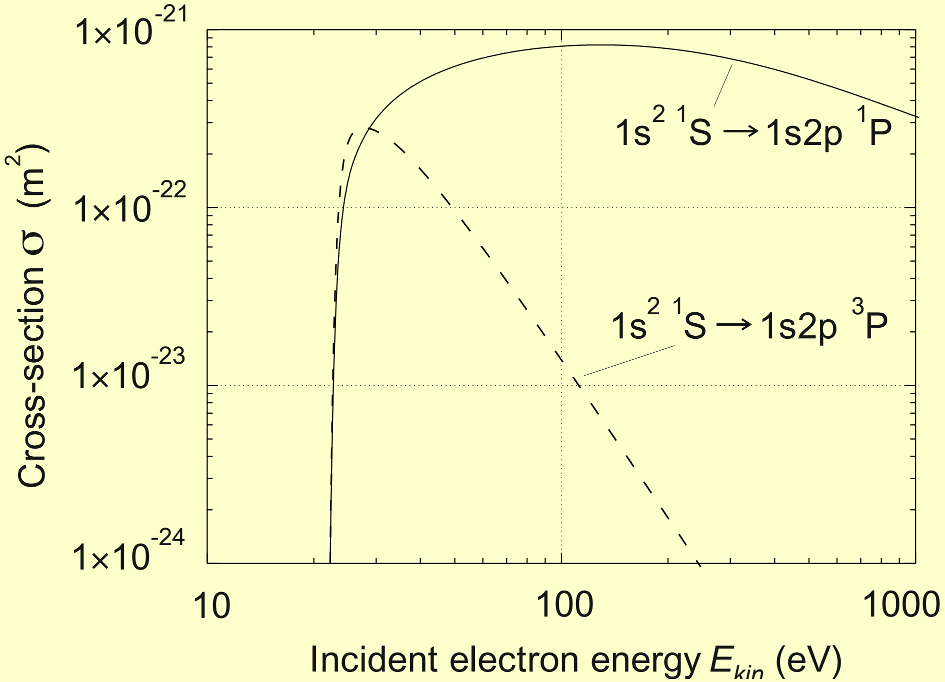

Furthermore, the cross-sections for excitation to the singlet and triplet levels differ strongly for high collision energies

$\longrightarrow$

Ratio of singlet to triplet lines well suited for T_e diagnostics ??

Pure corona model only holds for densities below $n_e \leq 10^{16}\ m^{-3}$

For higher densities collisions from the metastable levels to higher levels, between triplet and singlet levels, and ionization from the triplet levels become strong and all lines become also density dependent

Collisional radiative models which also include radiative transport were developed.

In this way pairs of lines in the visible spectral region were found which depend strongly only on one parameter, n_e or T_e, at least over a limited parameter range

Such methods have been used, for example, for studying the boundary region of fusion plasmas by injecting a He-beam

Table 10.1. Line pairs in He I suitable for diagnostics

	Transition	λ_1 (nm)	Transition	λ_2 (nm)	Parameter obtained
(a)	$3\,^3S \rightarrow 2\,^3P$	706.52	$3\,^1S \rightarrow 2\,^1P$	728.14	T_e
(b)	$3\,^1D \rightarrow 2\,^1S$	667.82	$3\,^1S \rightarrow 2\,^1P$	728.14	n_e
(c)	$4\,^3S \rightarrow 4\,^3P$	471.32	$4\,^1S \rightarrow 2\,^1P$	504.77	T_e

Attention should be paid to lines ending on the metastable levels $2\ ^1S$ *and* $2\ ^3S$ since they are the first ones to become affected by self-absorption

Spectra of highly ionized helium-like ions are heavily used in the diagnostics of fusion plasma

In the corona approximation
all electrons with energies above the excitation energy,
$E_{kin} > E_z(p) - E_z(g)$, participate in the excitation

The population densities and hence the emitted lines reflect correctly the energy distribution above threshold.

General inversion procedure is not possible.

One approach: One observes many lines with differing excitation energy,
takes an electron distribution function with few adjustable parameters and varies those till the population model fits the observations.

This was done in a neon glow discharge

An interesting variation: The emission from the vibrational levels of molecules in a nitrogen discharge was studied: it gave information on the low-energy part of the distribution function !

With increasing optical depth

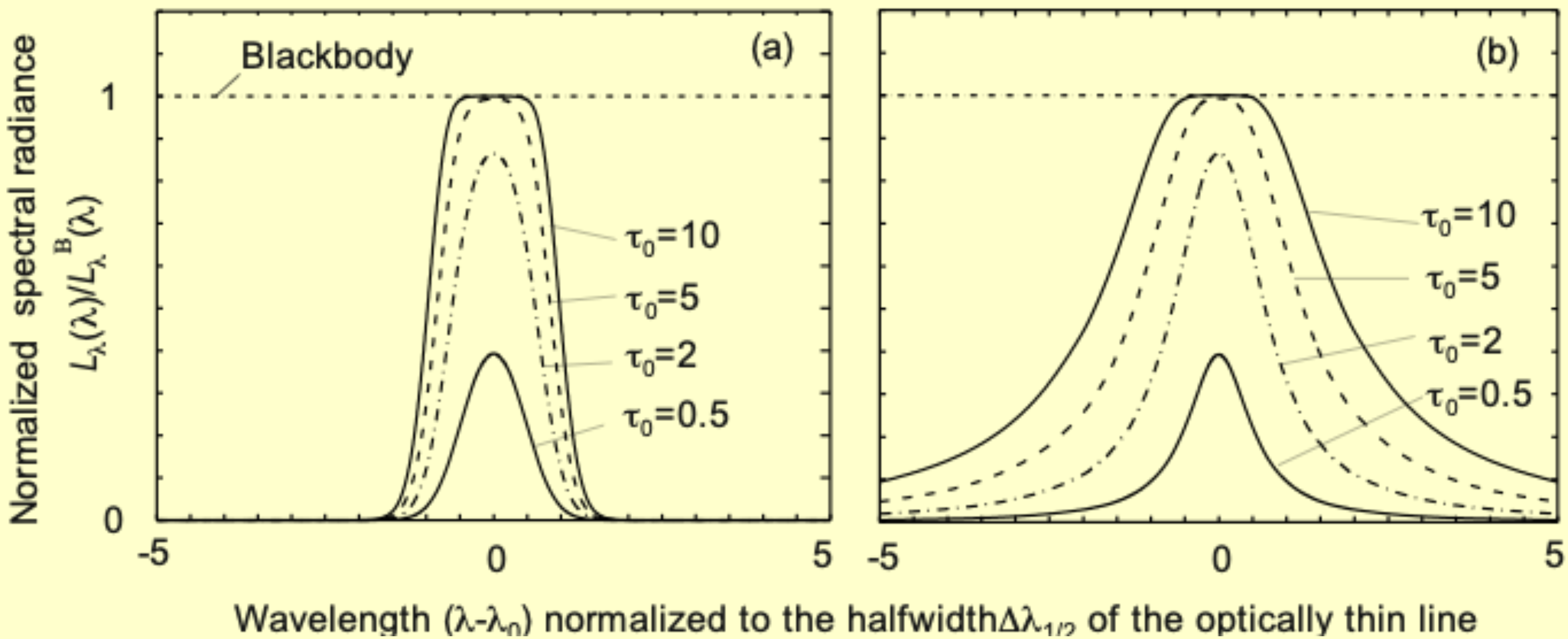

Gaussian

Lorentzian profile

The line approaches the blackbody limit, and the absolute value of the spectral radiance gives the temperature

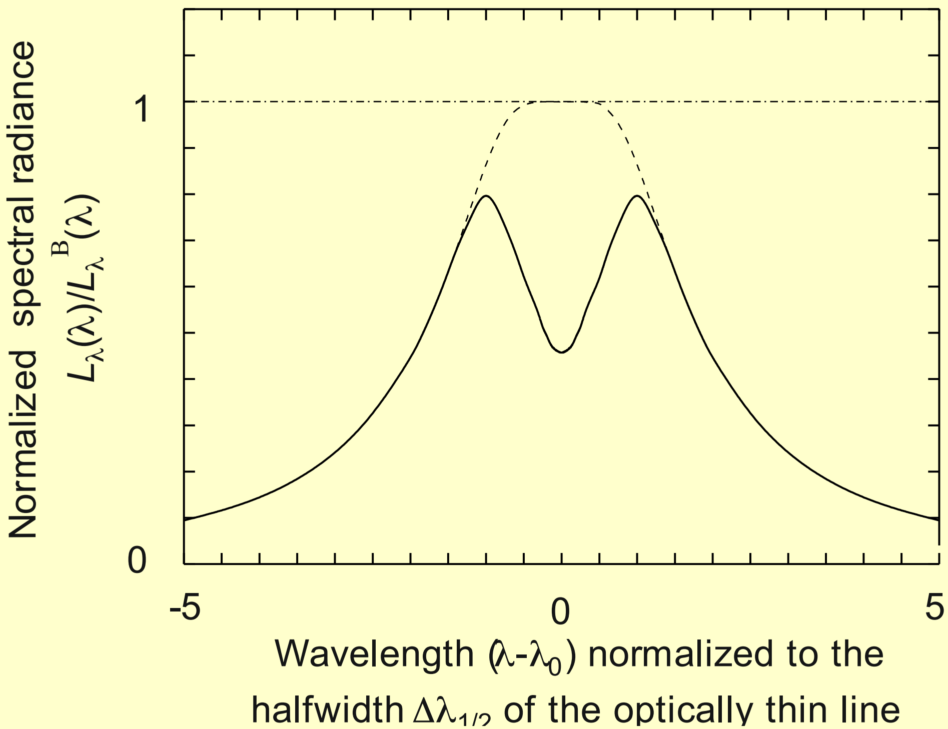

Lines from inhomogeneous plasmas can show a central dip caused by absorption in cooler boundary regions
→ *self-reversal*

The radiance of the two maxima $\approx$ 80% of the blackbody radiance at T_e, which exist at $\tau \approx 2$

Line to Continuum Ratio

This method is applicable to plasmas containing only hydrogenic and fully stripped ions

One selects lines with the upper level in PLTE with the bare nuclei, the population density is given by the Saha-Eggert equation, and bremsstrahlung and recombination radiation are also well known:

$$\frac{\varepsilon_z(p \rightarrow q)}{\int_{\lambda_{pq}-\Delta\lambda/2}^{\lambda_{pq}+\Delta\lambda/2} (\varepsilon^{ff} + \varepsilon^{fb}) \mathrm{d}\lambda} = f(T_e)$$

Advantage: No calibration of the optical system is necessary because one takes the continuum under the line!

If one takes a line ending at a level with high prinsipal quantum number n_q, ε^{fb} becomes neglible, since it scales with $1/n_q^3$.

At *low* T_e, the H^--continuum sets a limit, it depends on n_e

The method is applicable to helium plasmas above $T_e > 8$ eV and densities $n_e > 10^{20}\ m^{-3}$ when using the Paschen-β line at 320.3 nm

Recombination edges

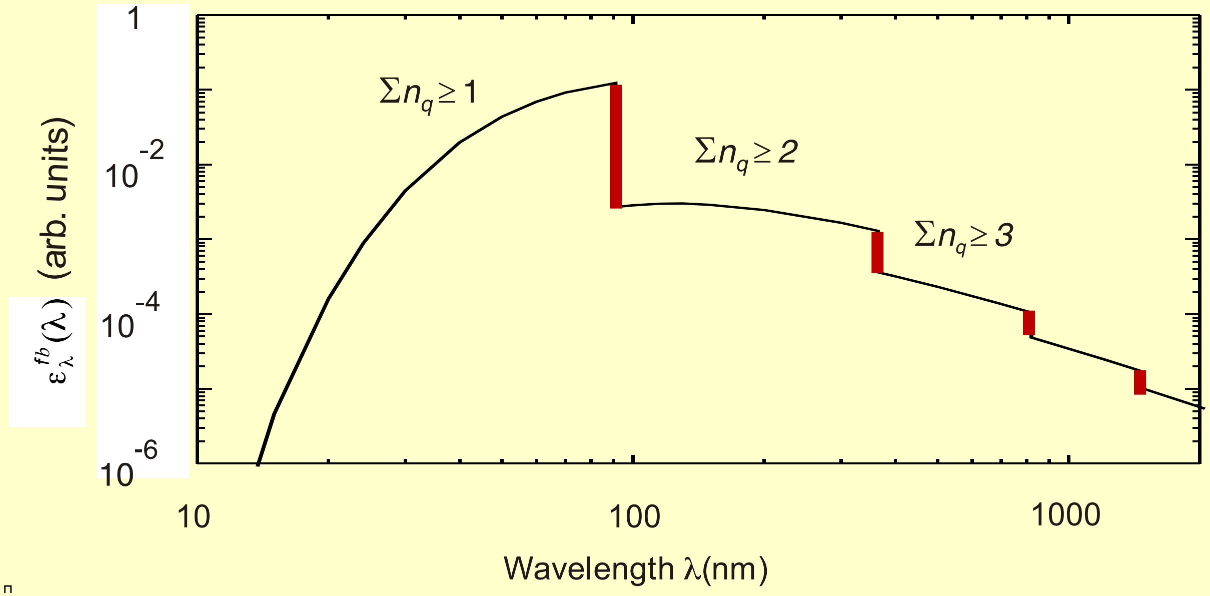

The ratio of the discontinuities is a function of T_e ,

is of limited applicability

Short- and Long-Wavelength Continuum

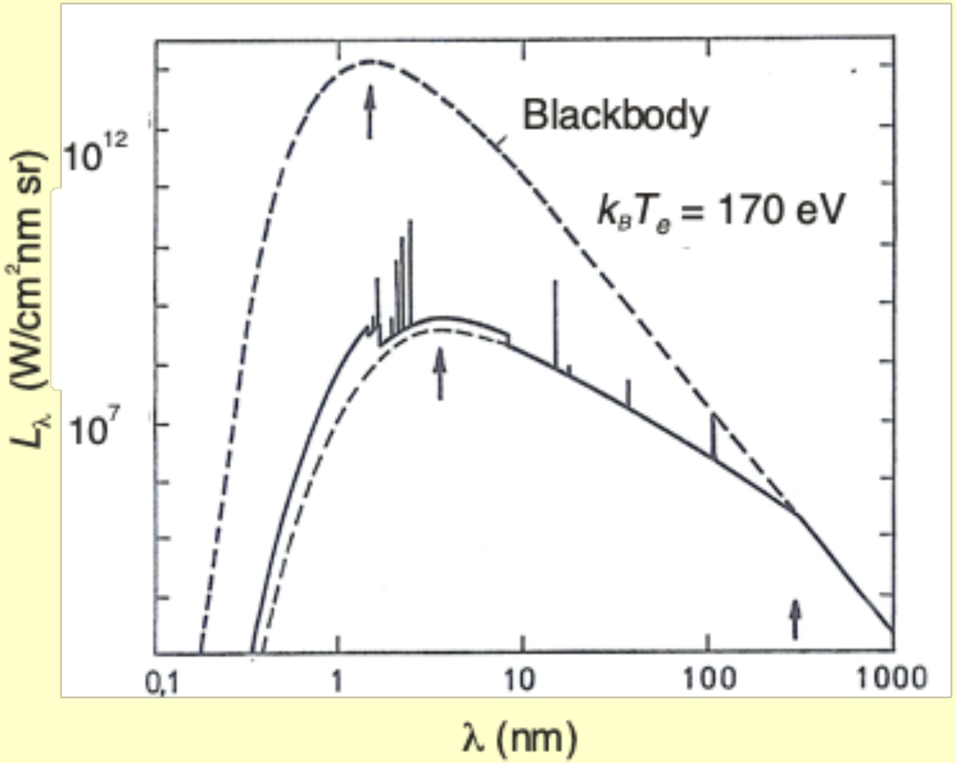

At long wavelengths

Only bremsstrahlung till the plasma becomes optically thick and the spectral radiance reaches the blackbody limit.

There T is obtained by either fitting the spectrum to a Planck function *or* measurement of the spectral radiance *absolutely* at *one* wavelength

At short wavelengths

$$both \quad \varepsilon_\nu^{ff} \text{ and } \varepsilon_\nu^{fb} \text{ are } prop \;\; e^{-\frac{h\nu}{k_B T}}$$

$$\text{i.e. } \log \varepsilon \sim -\frac{h}{k_B T}\,\nu$$

Straight line

Such spectra have been obtained in fusion plasmas with proportional counters

A general convenient approach:

Thin metallic foils properly selected are placed in front of the detectors
Metal and thickness of foils are chosen such that only very short wavelength radiation is transmitted.

The ratio of the transmitted radiation through two different foils is a sole function of T_e !

Sometimes called two-foil absorption method

Ratio of Ionzation Stages and Time Behavior

As we discussed yesterday, atomic species in a plasma go successively through their ionization stages till they reach ionization equilibrium (ionization = recombination)

or not in short-lived plasmas

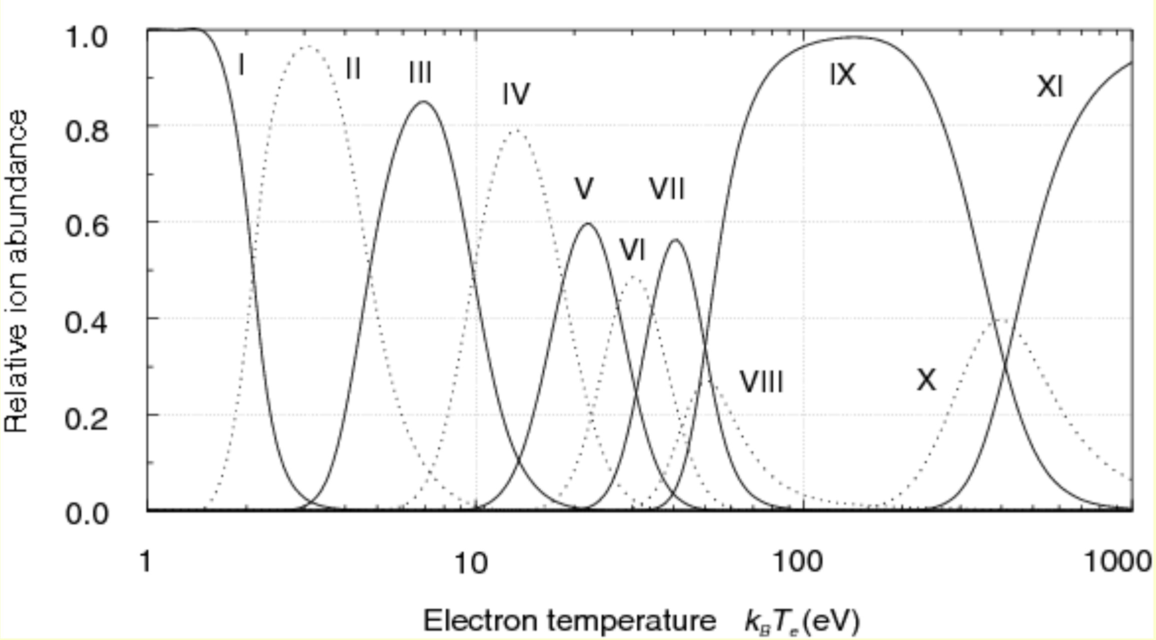

Each ionization stage exists in a temperature range around the temperature $T_{e,max}$ of maximum abundance.

This allows an estimate of T_e from the mere existence of an ion!

This is not meaningful at higher electron densities when density dependence sets in !

Measurements of the Electron Density

Electron Densities from Line Profiles

Line profiles are characterized by the shape, the width and the shift. Usually the width is used to derive the electron density.

It is common to use the Full Width at Half-Maximum (FWHM) designated by $\Delta\lambda_{1/2}$,

although in some theoretical calculations also the half half-width is given !

In principle, also the shift may be used for the density measurement but the shifts are usually less accurate.

The experimentally obtained profiles contain broadening by the Doppler effect and by the instrument function too, and the profile due to the plasma environment has to be retrieved by a de-convolution process

The experimental line shapes are usually rather well decribed by Voigt functions, which are the convolution of a Gaussian and a Lorentzian function

Gaussian:	Doppler broadening
Lorentzian:	Plasma broadening

Typical procedure: A theoretical Lorentzian profile is convolved with the instrument function and a Gaussian Doppler profile according to the atom/ion temperature and matched to the experimental profile by a least-square fit.

Important: Fitting of the total shape leads to a clear determination of the continuous background which is specifically crucial for lines with wide wings

Attention must be paid to lines ending on the ground state or a metastable level, since these lines are the first ones to become **optically thick**.

Stark broadening

(See lecture by Dr. Stambulchik)

Stark broadening of lines by electrons and ions usually dominates in plasmas.

The perturbation is by long-range Coulomb interaction
and the broadening hence is rather complex.
Interplay beween theory and experiment stimulated this field and lead to many data sets for diagnostic applications.

Bench-marking measurements increased their reliabilty !

Hydrogen and hydrogen-like ons

At ***low*** temperatures lines from hydrogen atoms are the most useful ones because of the large linear Stark effect, and
at ***high*** temperatures lines from hydrogen-like ions show sufficient broadening for the same reason

The Balmer lines of hydrogen are in the convenient visible spectral region.

The Balmer-beta line H_β at 486.13 nm is one of the most widely employed and extensively studied lines.

$$\frac{\Delta\lambda_{1/2}}{\mathrm{nm}} = 1.03 \times 10^{-15} \left(\frac{n_e}{\mathrm{m}^{-3}}\right)^{0.681}$$

Uncertainties of the half-width are below 10%.

The temperature dependence is weak, noticeable below 0.5 eV

High principal quantum number Balmer lines are useful candidates for radio frequency discharges ($n_e \approx 10^{19}\mathrm{m}^{-3}$) for edge plasmas of fusion devices ($n_e \approx 10^{21}\mathrm{m}^{-3}$)

Lines beween Rydberg levels are in the radio-frequency region and are used for density studies of interstellar plasmas

The next hydrogen-like ion is HeII, and the Paschen-α and Paschen-β lines at 468.56 nm and 320.31 nm, respectively, have been thoroughly studied too, both in experiments and Theory.

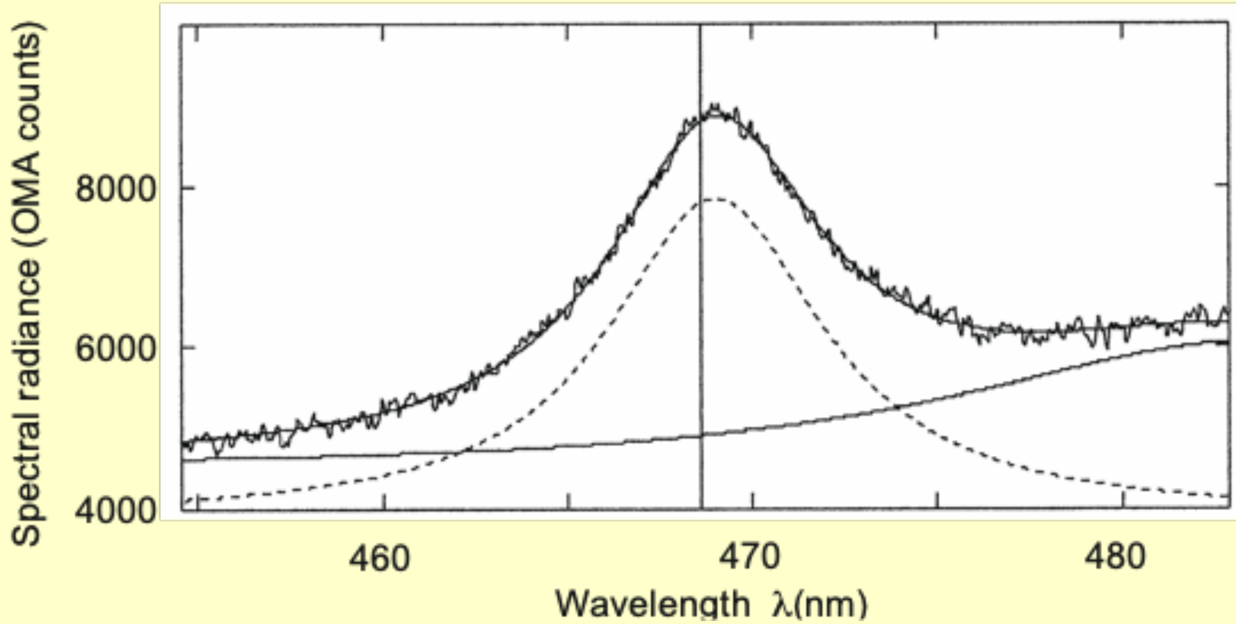

Here is an experimental profile of the P_α-line recorded from a plasma well diagnosed by Thomson scattering with

$$n_e = 3.5 \times 10^{24}\,\mathrm{m}^{-3} \quad \text{and} \quad k_B T_e = 6.8\ \mathrm{eV}$$

The full line shows the background and the dashed line gives the best-fit Voigt function

P_α-line: $$\frac{\Delta\lambda_{1/2}}{\mathrm{nm}} = 2.74\times 10^{-20} \left(\frac{n_e}{\mathrm{m}^{-3}}\right)^{0.831}$$

Accuracy about 10%*, weak temperature dependence*

Measuring the series of a line:

With increasing quantum number n_p of the upper level the lines become broader and move closer together as the level spacing decreases $\longrightarrow$ they overlap

Taking the width of several possible lines increases the accuracy of the density measurement !.

However, the *simple observation* of the last just observable line yields already a simple estimate of the perturber density n_z.

If $n_{p,max}$ is the principal quantum of the upper level of this line

$$\lg\frac{n_z}{m^{-3}} \approx 29.12 + 4.5 \lg Z - 1.5 \lg z - 7.5 \lg n_{p,max}$$

The relation is called Inglis-Teller limit

The following example shows the Lyman-α series of HeII emitted by a dense z-pinch

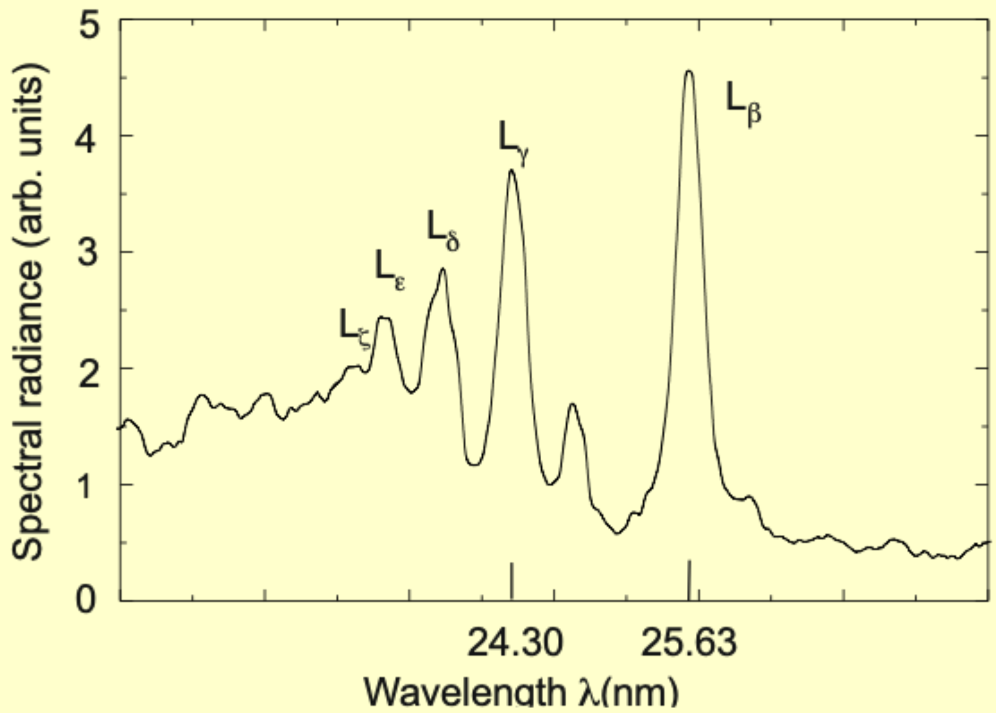

L_ε has $n_{p,mx} = 6$ → $n_z \approx 4.4 \times 10^{24} \mathrm{m}^{-3}$

Isolated Lines of Atoms and Ions

Broadening of well-isolated lines is pedominantly by electron impact with small contributions due to the quadratic Stark effect by the microfield

Numerous theoretical calculations and experimental observations have been done and the diagnostician simply has to consult respective data banks (See lecture by Dr. Stambulchik)

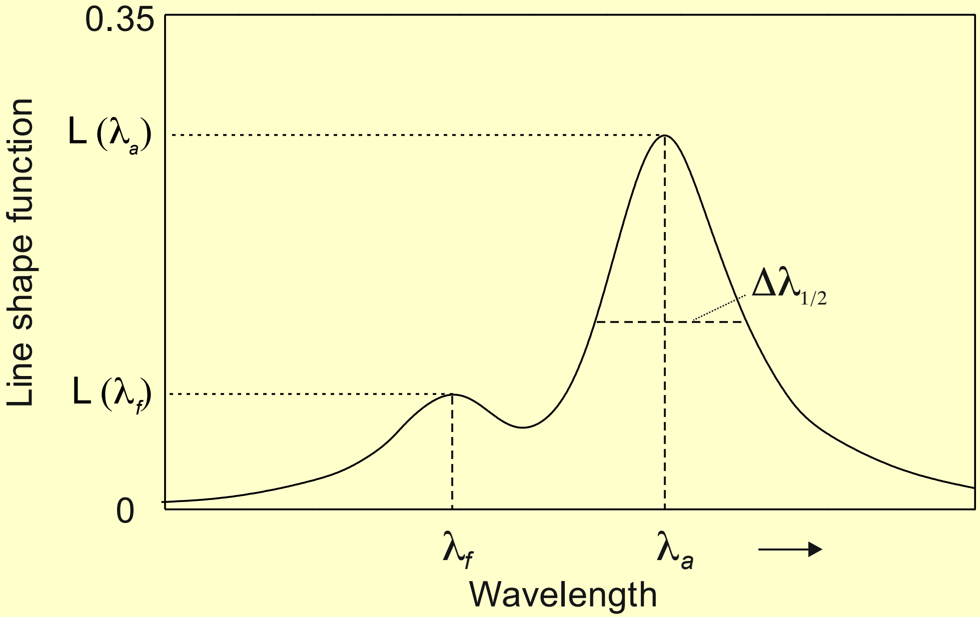

An interesting possiblity offer lines with a close-by forbidden component, for example, HeI lines

With increasing electron density the upper levels mix by the electric field and the ratio of allowed and forbidden component changes

For the ratio of the $4\ ^3D,\ ^3F \rightarrow 2\ ^3P$ transitions, for example,

$$\frac{\varepsilon(\lambda_f)}{\varepsilon(\lambda_a)} \approx 6 \times 10^{-23}\ \frac{n_e}{\mathrm{m}^{-3}}$$

This ratio alone yields already the density,
although fitting the whole profile leads to much higher accuracy

Electron Densities from the Ratio of Lines

One selects two lines of an ion:

the upper level of one line decays only radiatively,
the upper level of the second line decays *in addition*
by collisions to other levels and by ionization

$R = \varepsilon_1/\varepsilon_2 \approx f(n_e)$ over some limited temperature range

The upper level of the second line is in most cases a metastable level.

Typical candidates are helium-like ions,

but suitable line pairs have also been found in argon and for the ions of the isoelectronic sequencies of

boron, nitrogen, oxygen, sodium and copper, and in nickel-like tungsten

Electron Density from the Continuum Emission at Long Wavelength

Bremsstrahlung at long wavelength of fully stripped ions

$$\varepsilon_{\lambda}^{ff}(\lambda) \sim \frac{n_e^2}{\sqrt{T_e}}$$

i.e. it is a strong function of n_e and a weak function of T_e

A crude knowledge of T_e thus allows good measurements of n_e !

A couple of other density diagnostics are available but not widely applicable and in most cases of lower accuracy

Examples:

In plasmas heated rapidly to high temperatures the ions go successively through the ionizations stages, the decay time τ_z being given by

$$\tau_z = \frac{1}{n_e S_z}$$

Since at high T_e the ionization rate coefficient S_z is practically independent of T_e, the electron density determines the decay.

Diagnotics of the boundary plasma in fusion-oriented plasmas by injection of thermal and superthermal beams
e.g. He- and Li-beams

Measurement of Magnetic fields

From the magnetic field one also gets the *current* density via the fourth Maxwell equation $\mu_0 \boldsymbol{j} = \nabla \boldsymbol{B}$

The magnetic fields splits the energy levels of atomic systems and hence the emitted lines by the Zeeman effect. The Doppler effect at high temperature and the Stark effect at high densities broaden the components. To use the polarization properties of the components can help.

Long-wave lines of *heavy* ions like the magnetic dipole lines were successful employed.

A novel interesting approach was advanced not too long ago: Fine structure components experience the same Doppler and Stark broadening but different Zeeman splitting $\longrightarrow$ the different line widths lead to $\boldsymbol{B}$!

Motional Stark effect

Energetic neutral atoms injected at very high energies into the plasma experience in their rest frame a Lorentz electric field

$$\mathbf{E} = \mathbf{v} \times \mathbf{B}$$

Hence Stark splitting gives information on the B-field.

Electric fields

Electric fields are measured in principle by the Stark effect on emitted lines

The always present plasma field gives the broadening.

The directed fields in front of electrodes may be sufficient to split Rydberg levels

Strong turbulent fields lead to additional broadening in the lines of hydrogen and hydrogen-like ions and have been studied this way.

High-frequency electric fields produce satellite transitions shifted by the angular frequency ω, 3ω, ...around a forbidden transition, and by 2ω, 4ω,… around an allowed line

Ultimate ideal goal:

Collisional radiative models for the atoms and ions and best fit to as many as possible lines $\longrightarrow$ n_e *and* T_e

(partly available for He and Ar)

Material is from *Introduction to Plasma Spectroscopy*